Coulomb Bicrystals of Species with Identical Charge-to-Mass Ratios

T. Matthey[1] and J. P. Hansen[2]

[1]*Parallab, Department of Informatics, P.O. Box 7800, University of Bergen, 5007 Bergen, Norway*
[2]*Department of Physics, P.O. Box 7800, University of Bergen, 5007 Bergen, Norway*

M. Drewsen

QUANTOP–Danish National Research Foundation Center for Quantum Optics and Department of Physics and Astronomy,
University of Aarhus, 8000 Aarhus C, Denmark
(Received 3 April 2003; published 16 October 2003)

Structures of cold bicomponent Coulomb systems of particles with identical charge-to-mass ratios and common oscillation frequency in a spherical harmonic potential are studied by molecular dynamics simulations with up to 10^6 particles. For most initial conditions and cooling rates, the final state becomes a completely mixed core surrounded by a set of nearly degenerated double shells of separate species. For an equal amount of the two species, it is found that the ground state for larger systems consists of a simple cubic structured core surrounded by outer double-shell structures.

Confined classical Coulomb systems of identical charged particles have been intensively studied theoretically in the low temperature limit during the past decades. These investigations have led to a wide range of important results for single component systems including determination of the ground state transition temperature of infinite systems [1] and characterization of the structures of finite systems under various confinement conditions (see, e.g., [2] and references therein). Ion traps in combination with laser cooling have in recent years offered the possibility to experimentally test theoretical predictions by studying condensed single component systems of positive atomic ions. Among the striking results are observations of real translational symmetric crystalline structures in large ion systems of $\gtrsim 10^5$ ions in Penning traps [3,4] and large cylindrical crystal structures in rf traps [5,6]. Besides being interesting systems within condensed matter and plasma physics, crystalline ion ensembles are interesting objects for such diverse fields as accelerator physics [7,8], quantum computing [9], and astrophysics [10].

Two-component systems have been considered theoretically earlier in a few investigations [11–16] mostly dedicated to confinement conditions equivalent to that of the Penning trap [11–15]. In connection with recent experiments on bicrystal structures of singly charged ions with different masses in linear Paul traps [17], specific simulations of smaller systems up to a few thousand ions have been made [16]. Two-component systems are, however, a very rich field for theoretical research with importance for development of experiments utilizing bicrystals such as cold molecular ion studies [18,19] and other experiments involving sympathetically cooled ions [15,20]. For studies involving particles with identical or near identical charge-to-mass ratios $\frac{q}{m}$, results may furthermore be very relevant for understanding the cooling process of white dwarf stars [10].

In this Letter we consider the spatial ordered structures of two-component systems of particles with identical charge-to-mass ratios $\frac{q}{m}$ and common oscillation frequency in a spherical harmonic trapping potential at low temperatures. The considered trapping condition can effectively be realized in both Penning and Paul traps, and the spherical geometry makes it possible to compare the results with previous [21,22] as well as new simulations of single component systems in a similar simple spherical geometry. More specifically, we will focus our presentation on the case where $q_2 = 2q_1$ and $m_2 = 2m_1$.

The total potential energy of an N ion system of the type defined above is simply given by

$$U = \sum_{i=1, j>i}^{N} \frac{Q_i Q_j}{|\vec{r}_i - \vec{r}_j|} + \frac{1}{2} \sum_{i=1}^{N} M_i \omega^2 \vec{r}_i^2, \qquad (1)$$

where M_i and Q_i are the mass and charge of particle i, respectively, and ω is the common effective trap frequency.

For identical particles, e.g., particles characterized by (q, m), it has earlier been found that such systems typically reach a solid state phase when $\Gamma = \frac{q^2}{a k_B T} \gtrsim 200$, where $a = [q^2/(m\omega^2)]^{1/3}$ is the Wigner-Seitz radius for maximum density and T is the temperature [1,23]. In general, for a two-component system, two coupling parameters may be introduced. For simplicity, we will state only the one, Γ_1, corresponding to particles characterized by (q_1, m_1) since at thermal equilibrium $\Gamma_2 = 2^{5/3}\Gamma_1$.

In the present molecular dynamics (MD) approach, we solve Newton's equation, $M_i \frac{d^2}{dt^2} \vec{r}_i(t) = \vec{F}_i(t)$ for a variable number of particles up to 10^6. The simulations were performed with PROTOMOL [24], an object-oriented component-based MD framework. The equations of motion of the particles are propagated by a leapfrog integrator scheme with a Nosé-Hoover thermostat. With a typical value of $\Gamma_1 \sim 1$ for the initial phase, the ions are cooled

down to a temperature corresponding to $\Gamma_1 \approx 10^6$ or larger. The cooling period is $4 \times 10^5 \omega^{-1}$, and the integration time step is $0.004\omega^{-1}$ or less. The Coulomb part is computed directly for the smallest systems with $N \leq 20\,288$, whereas a multigrid method [25,26] is used for systems with $N > 20\,288$. The processing speed for the multigrid method is up to a factor of ~ 1000 larger than the direct method when $N = 10^6$, with the cost of introducing a relative energy error of the order of 10^{-5} or less. No significant discrepancies are found in structures and energies between the multigrid and the direct calculations in the transition region around $20\,288$ ions when considering initially disordered states. For all final configuration energies the Coulomb part is computed by direct summation.

In Fig. 1, the radial particle density distributions of two 50%:50% bicomponent systems are compared with corresponding distributions from monocomponent systems. In all simulations the final value of Γ_1 exceeded 10^6. Since the space charge limited density of particles characterized by (q, m) in the potential given by Eq. (1) is proportional to m/q^2, the bicrystal has a larger radius than its monocomponent counterpart of particles with parameters (q_1, m_1). Qualitatively, both systems look surprisingly similar with a number of outer shells sur-

rounding a homogeneous inner charge distribution. Quantitatively, the shells of the bicomponent system appear however to be fewer and more diffuse. In order to explore these findings in detail, we show in the inset of Fig. 1 the outer parts of the radial density distribution of each component. It is observed that the two species are uniformly mixed throughout the crystal with each shell containing a nearly identical number of each species. The fact that the two species completely mix can be understood by the following simple electrostatic argument: For a particle with charge q and mass m confined by a spherical harmonic potential with oscillation frequency ω, the equilibrium position outside a centrally positioned spherical uniform charge distribution with total charge Q is proportional to $(\frac{Qq}{\omega^2 m})^{1/3}$. Hence the position will be the same for particles with identical q/m, and a strong mixing can be expected.

A close inspection of the insets of Fig. 1 indicate, however, a small splitting of each shell, with the heaviest particles occupying the inner part. The splitting δr is obviously constant and nearly independent of the system size. Furthermore, δr is empirically found to be in agreement with

$$\delta r \approx a_2 - a_1, \tag{2}$$

where a_1 and a_2 are the Wigner-Seitz radii for pure systems of (q_1, m_1) and (q_2, m_2) particles, respectively. This result has been found to be valid for other mixture ratios and for other (q_2, m_2) particles satisfying $q_2/m_2 = q_1/m_1$ as well.

In order to compare the outer intrashell structures of a monocomponent cold system with a bicomponent one, in Fig. 2, projections of the outer shell hemispheres of systems containing $20\,288$ (q_1, m_1) particles and $10\,144$ $(q_1, m_1) + 10\,144$ (q_2, m_2) particles are presented. While the monocomponent system clearly exhibits regular hexagonal lattice structure, the bicomponent structure is highly disordered with only very short range correlations. This fact is distilled in the lower part of Fig. 2, where the pair correlation functions for the interparticle distances of the outer shell for three cold systems are displayed. The two monocomponent systems show very high and sharp nearest neighbor correlations as well as peaks corresponding to long range correlations of an ideal 2D hexagonal lattice. At least peaks indicating the positions of the sixth nearest neighbors are observed. In contrast, the bicomponent pair correlation function shows only short range correlations and the present peaks are significantly broader. The interesting three-hump structure of the nearest neighbor peak in the bicrystal correlation function can be understood on the basis of the nearest neighbor distances between identical particles of the two species and the typical minimum distance between the two particles of different species.

The energy ground state for single component systems confined by a spherical harmonic potential has previously been investigated as a function of particle numbers in
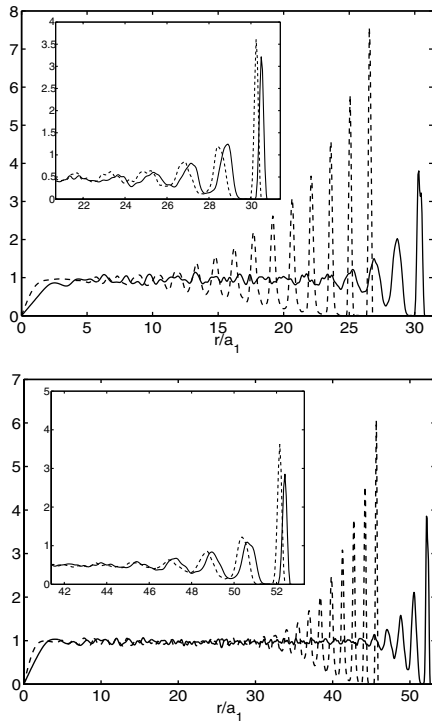
FIG. 1. Radial density distributions of cold monocomponent (dashed lines) and bicomponent (solid lines) systems. Insets illustrate the outer density distributions of the two species, (q_1, m_1) (solid lines) and (q_2, m_2) (dashed lines). Upper graph: $20\,288$ (q_1, m_1) particles and $10\,144$ $(q_1, m_1) + 10\,144$ (q_2, m_2) particles. Lower graph: $100\,000$ (q_1, m_1) particles and $50\,000$ $(q_1, m_1) + 50\,000$ (q_2, m_2) particles.
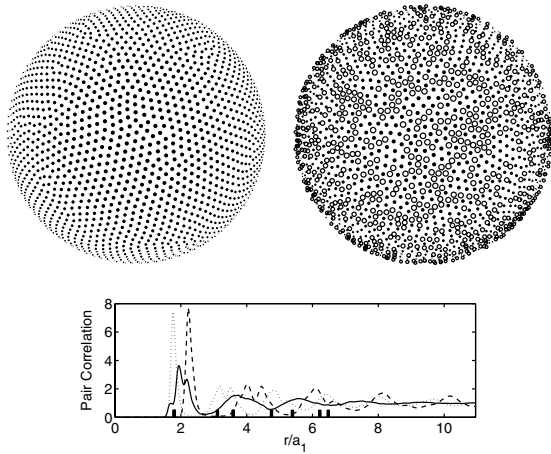
FIG. 2.　2D projections of the hemispheres of the outer shell of systems containing 20 288 (q_1, m_1) particles (upper left), and 10 144 (q_1, m_1) (●) +10 144 (q_2, m_2) particles (○) (upper right). The 2D pair correlation function of monocomponent and bicomponent crystals for the outermost shell is presented for 20 288 (q_1, m_1) particles (dotted line), 20 288 (q_2, m_2) particles (dashed line), and 10 144 (q_1, m_1) + 10 144 (q_2, m_2) particles (solid line) are shown in the lower panel. Solid boxes represent plane 2D hexagonal lattice pair correlation positions for (q_1, m_1) particles.

MD surveys by calculating the cohesive energy of cold systems developing from various initial configurations and temperatures [21,22]. In Fig. 3, we present the calculated cohesive energies for a series of MD simulations of 50%:50% mixed bicomponent systems of various sizes. The calculated average cohesive energy per particle is given by

$$U_{\text{coh}} = (U - U_{\text{homo}})/(N\tilde{q}^2/\tilde{a}). \qquad (3)$$

Here, U is the actual Coulomb energy of the system and $U_{\text{homo}} = 9/10 N^{5/3}(\tilde{q}^2/\tilde{a})$ is the energy of an equivalent homogeneous charge distribution, based on particles of a charge $\tilde{q} = \frac{1}{2}(q_1 + q_2)$, and a corresponding effective Wigner-Seitz radius $\tilde{a}$ given by

$$\tilde{a} = \left(\eta_1 \frac{q_1^2}{m_1 \omega^2} + \eta_2 \frac{q_2^2}{m_2 \omega^2} \right)^{1/3} = (\eta_1 a_1^3 + \eta_2 a_2^3)^{1/3}, \qquad (4)$$

where η_1 and η_2 denote the relative content of the two species in the system (this definition will be justified below).

As seen from Fig. 3, for up to around $N = 2500$ particles, the cohesive energy does not depend critically on the initial condition. As a result, the final state always becomes a crystalline state with the particles arranged in nearly concentric double shells. However, for systems with a larger number of particles, an initial spherical truncated simple cubic (sc) structure with one (q_1, m_1) particle and one (q_2, m_2) particle forming a basis pair oriented along the [111] direction gives rise to a lower value of U_{coh} than other initial spherically truncated
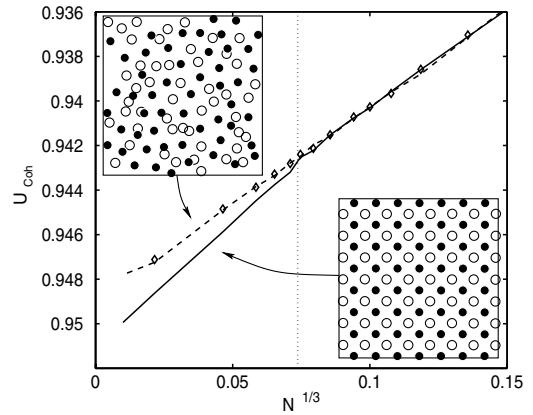
FIG. 3.　Cohesive energy U_{coh} of 50%:50% (q_1, m_1)-(q_2, m_2) cold bicomponent systems obtained from MD simulations with different initial structures and various number of particles N: Spherical truncated fcc structure (◇) with one (q_1, m_1) particle and one (q_2, m_2) particle forming a basis pair oriented along one of the main crystal axes, spherical truncated simple cubic (sc) structure (solid line) with one (q_1, m_1) particle and one (q_2, m_2) particle forming a basis pair oriented along the [111] direction, and a disordered state (dashed line). The vertical dotted line at $N \approx 2\,500$ indicates an estimate of the minimum number of particles needed for a system with clusters of sc structures to become energetically favorable. The insets show the projection of "fluid" and sc structures for a layer of thickness $1.1 a_1$ in the center of systems with $N = 20\,288$.

crystalline structures or disordered states. By a detailed analysis of the final particle distributions of larger particle ensembles, we find that in the case of an initial sc structure, clusters of sc structures remain already when N exceeds ~2500, and from the largest simulated systems with $N = 10^6$, the main part of the crystal remains in a sc structure, indicating that the ground state of an infinite system will be a sc structure. The insets of Fig. 3 present projection of central regions of crystals with $N = 20\,288$ particles. Here the characteristics of fluid and sc structures are clearly seen.

The introduced effective Wigner-Seitz radius $\tilde{a}$ in Eq. (4) can be justified by the results presented in Fig. 4. In Fig. 4(a) the values given by Eq. (4) are compared with values derived from MD simulations. The plot considers two sets of simulations for systems ranging from 10^2 to 10^6 particles with $\eta_1, \eta_2 = 0.5$ and $\eta_1 = 1$, respectively. The results indicate that Eq. (4) is a reasonable definition for an effective Wigner-Seitz radius. The validity of Eq. (4) is furthermore supported by Fig. 4(b), where values of $\tilde{a}$ calculated by Eq. (4) are compared with the simulated value for various values of η_1. Again a nearly perfect agreement is found.

The presented work has thus far been focused on very cold systems with $m_2 = 2m_1$ and $q_2 = 2q_1$, but several less systematic series of simulations on cold systems with $m_2 = p \cdot m_1$ and $q_2 = p \cdot q_1$, where $p = 3, 4, 5$ and 8 give the same main conclusions, including the
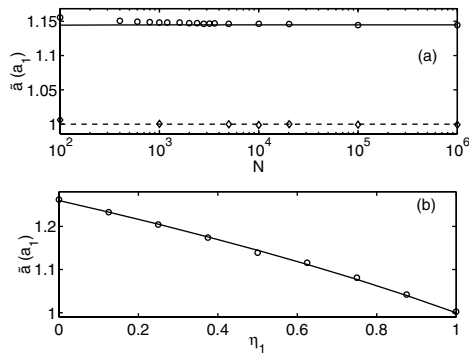
FIG. 4.   (a) Wigner-Seitz radii deduced from simulations for pure N (q_1, m_1) particle systems ($\diamondsuit$) and for mixed systems with an equal amount of (q_1, m_1) and (q_2, m_2) particles ($\bigcirc$). The solid and dashed lines are the corresponding predicted Wigner-Seitz radius from Eq. (4). (b) The effective Wigner-Seitz radii given by Eq. (4) (solid line) and derived from simulations of systems consisting of 20 288 particles ($\bigcirc$) for various values of η_1.

results represented by Eqs. (2) and (4). We have furthermore performed several simulations to test the sensitivity of the mixing on the charge-to-mass ratio of the two particle types, and we have found that a difference of one per thousand is enough to observe at least partial segregation of the two species. The structural development that appears when cooling bicomponent systems down to the very low temperatures considered in the present Letter is an interesting issue to study in the future.

In summary, we have shown that the ground state of two-component particle systems with identical charge-to-mass ratios consists of a number of double structured shells surrounding a mixed inner core. The sc structure is the ground state of an infinite 50%:50% system. For the specific case of m_1, q_1 and $m_2 = 2m_1$, $q_2 = 2q_1$, we have found for a particle number larger than ∼2500 that clusters of sc structures in the core are energetically favorable. Finally, we have shown that on a coarse scale (larger than the Wigner-Seitz radius), the two species mix completely independent of the relative abundances. This has led to a definition of a single effective Wigner-Seitz radius for bicomponent systems.

[1] E. L. Pollock and J. P. Hansen, Phys. Rev. A **8**, 3110 (1973).
[2] D. H. E. Dubin and T. M. O'Neil, Rev. Mod. Phys. **71**, 87 (1999).
[3] W. M. Itano, J. J. Bollinger, J. N. Tan, B. Jelenkovic, X.-P. Huang, and D. J. Wineland, Science **279**, 686 (1998).
[4] T. B. Mitchell, J. J. Bollinger, D. H. E. Dubin, X.-P. Huang, W. M. Itano, and R. H. Baughman, Science **282**, 290 (1998).
[5] G. Birkl, S. Kassner, and H. Walther, Nature (London) **357**, 310 (1992).
[6] M. Drewsen, C. Brodersen, L. Hornekær, J. S. Hangst, and J. P. Schiffer, Phys. Rev. Lett. **81**, 2878 (1998).
[7] A. Rahman and J. P. Schiffer, Phys. Rev. Lett. **57**, 1133 (1986).
[8] R. W. Hasse, Phys. Rev. Lett. **86**, 3028 (2001).
[9] J. I. Cirac and P. Zoller, Phys. Rev. Lett. **74**, 4091 (1995).
[10] J. L. Barrat, J. P. Hansen, and R. Mochkovitch, Astron. Astrophys. **199**, L15 (1988).
[11] T. M. O'Neil, Phys. Fluids **24**, 1447 (1981).
[12] D. J. Larson, J. C. Bergquist, W. M. Itano, and D. J. Wineland, Phys. Rev. Lett. **57**, 70 (1986).
[13] J. P. Schiffer, in *Proceedings of the Workshop on Crystaline Ion Beams, Wertheim, Germany, 1988*, editedy by R. W. Hasse, I. Hofmann, and D. Liesen (GSI Report No. GSI-89-10, 1989).
[14] H. Imajo, K. Hayasaka, R. Ohmukai, U. Tanaka, M. Watanabe, and S. Urabe, Phys. Rev. A **55**, 1276 (1997).
[15] L. Gruber, J. P. Holder, J. Steiger, B. R. Beck, H. E. DeWitt, J. Glassman, J. W. McDonald, D. A. Church, and D. Schneider, Phys. Rev. Lett. **86**, 636 (2001).
[16] L. Hornekær, Ph.D. thesis, University of Aarhus, Denmark, 2000.
[17] L. Hornekær, N. Kjærgaard, A. M. Thommesen, and M. Drewsen, Phys. Rev. Lett. **86**, 1994 (2001).
[18] K. Mølhave and M. Drewsen, Phys. Rev. A **62**, 011401 (2000).
[19] I. S. Vogelius, L. B. Madsen, and M. Drewsen, Phys. Rev. Lett. **89**, 173003 (2002).
[20] D. Kielpinski, B. E. King, C. J. Myatt, C. A. Sackett, Q. A. Turchette, W. M. Itano, C. Monroe, D. J. Wineland, and W. H. Zurek, Phys. Rev. A **61**, 032310 (2000).
[21] R. H. Hasse and V. V. Avilov, Phys. Rev. A **44**, 4506 (1991).
[22] H. Totsuji, T. Kishimoto, C. Totsuji, and K. Tsuruta, Phys. Rev. Lett. **88**, 125002 (2002).
[23] D. H. E. Dubin and T. M. O'Neil, Phys. Rev. Lett. **60**, 511 (1988).
[24] J. A. Izaguirre, J. Willcock, T. Matthey, Q. Ma, T. B. Slabach, T. Steinbach, S. Stender, G. F. Viamontes, and J. Mohnke. PROTOMOL: An object-oriented framework for molecular dynamics. Available online via http://protomol.sourceforge.net (2000–2003).
[25] T. Matthey, Ph.D. thesis, University of Bergen, Norway, 2002.
[26] B. Sandak, J. Comput. Chem. **22**, 717 (2001).